EUROPEAN ORGANIZATION FOR NUCLEAR RESEARCH
European Laboratory for Particle Physics

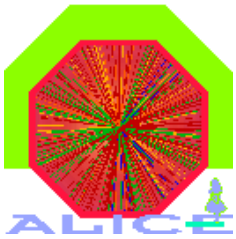

Internal Note/Physics
ALICE reference number
ALICE-INT-2006-015 version 1.0

Date of last change
12.07.06

Study of the ALICE performance for the measurement of beauty production in pp collisions at √s = 14 TeV via displaced electrons

Authors:

F.Antinori, C.Bombonati, M.Lunardon
Università degli Studi di Padova and INFN – Sezione di Padova, Padova, Italy

A.Dainese
INFN – LNL, Legnaro (PD), Italy

Abstract:

The study of beauty production in pp collisions at LHC energy has a large interest as a testing ground for perturbative QCD in a new energy domain and as a reference for investigating, in Pb-Pb collisions, medium effects on the propagation of heavy quarks. We present the results of a simulation study aimed at preparing a strategy for the selection of electrons from beauty decays in the ALICE central barrel.

1 Introduction

The primary physics goal of the ALICE experiment [1] is the study of the properties of QCD matter at the energy densities of several hundred times the density of atomic nuclei that will be reached in central Pb–Pb collisions at the LHC ($\sqrt{s_{\rm NN}}$ = 5.5 TeV). Under these conditions a deconfined state of quarks and gluons is expected to be formed. Heavy quarks, and hard partons propagating through the medium will allow us to probe its properties. For instance, measuring a high transverse momentum ($p_{\rm t}$) suppression of beauty hadrons should allow to investigate the predicted quark-mass dependence of parton energy loss [2]. In this context, the measurement of the beauty $p_{\rm t}$-differential cross section in pp collisions serves as "vacuum" reference for the study of medium effects in nucleus–nucleus collisions.

We stress, however, that the measurement of beauty production in pp collisions at the next collider-energy frontier, $\sqrt{s}$ = 14 TeV, is an important item *per se*, since it will allow to test and further improve perturbative QCD (pQCD) calculations. At Tevatron energy ($\sqrt{s}$ = 1.8 and 1.96 TeV), the disagreement between data and theory concerning beauty production has been reconciled after about 15 years from the first measurements, and has stimulated significant progress on both the experimental and the theoretical side (see e.g. [3, 4]). ALICE can carry out a sensitive measurement of beauty production over a large kinematic acceptance: at central rapidity (e.g. via displaced electrons, as we discuss in this work) and at forward rapidity (via muons [5]), and with a low cutoff in transverse momentum. These features should allow ALICE to be competitive with the pp-dedicated LHC experiments on the measurement of beauty production. Note, also, that pQCD calculations will have to be used to scale the beauty cross section in pp, measured at 14 TeV, to the Pb–Pb centre-of-mass energy of 5.5 TeV. For this reason it will be mandatory to validate the calculations both at Tevatron and LHC energies.

For the performance study presented here, we assume the baseline heavy-flavour production cross sections and yields presented in Table 1 (from the ALICE Physics Performance Report, Volume II [6]). These values are obtained from the pQCD calculation at fixed, next-to-leading, order (FO NLO) implemented in the HVQMNR program [7]; for the quark masses and factorization and renormalization scales, we used: $m_{\rm c}$ = 1.2 GeV and $\mu_F = \mu_R = 2\,m_{\rm t,c}$ for charm (where $m_{\rm t,c} = \sqrt{p_{\rm t,c}^2 + m_{\rm c}^2}$), $m_{\rm b}$ = 4.75 GeV and $\mu_F = \mu_R = m_{\rm t,b}$ for beauty; we averaged the results obtained with two sets of parton distribution functions, CTEQ 5M1 [8] and MRST HO [9]. Note that these cross sections have a theoretical uncertainty of the order of a factor 2 [6]. The yields, expressed as number of pairs per inelastic collision, are evaluated assuming an inelastic pp cross section of 70 mb at $\sqrt{s}$ = 14 TeV [1].

Beauty detection via electron-identified tracks with a displacement with respect

Table 1: NLO calculation results [7] for the $\rm c\overline{c}$ and $\rm b\overline{b}$ production cross sections and yields in pp collisions at $\sqrt{s}$ = 14 TeV (see text for details). Lower rows: yields of decay electrons.

	Charm	Beauty	
$\sigma^{\rm Q\overline{Q}}$ [mb]	11.2	0.51	
$N^{\rm Q\overline{Q}}$	1.6×10^{-1}	7.2×10^{-3}	
decay electrons	3.2×10^{-2}	1.6×10^{-3}	$(+1.4 \times 10^{-3})_{\rm b\to c\to}e$
decay electrons in $\lvert\eta\rvert < 0.9$	8.0×10^{-3}	4.0×10^{-4}	$(+3.5 \times 10^{-4})_{\rm b\to c\to}e$

to the primary collision vertex is favoured by the large semi-electronic branching ratio (b.r. $\approx 11\%$ [10]) and by the significant mean proper decay length ($c\tau \approx 500$ μm [10]) of beauty hadrons. The ALICE experiment has been designed also in view of exploiting these features. The central barrel ($|\eta| < 0.9$) provides good capabilities for electron identification in the Transition Radiation Detector (TRD) and in the Time Projection Chamber (TPC), coupled to precise tracking and vertexing in the TPC and in the silicon detectors (pixels, drifts and strips) of the Inner Tracking System (ITS). In the lower rows of Table 1 we report the number of charm and beauty decay electrons per event, in the full solid angle and in the barrel acceptance. In addition to direct semi-electronic decays, beauty hadrons can decay indirectly to an electron via a charm hadron (e.g. B $\rightarrow$ D $\rightarrow e + X$); these chain decays have a b.r. of $\approx 10\%$. The $p_{\rm t}$ distribution of these electrons is much softer than that of electrons from direct beauty decays. In Table 1, this contribution is reported in parenthesis. As we discuss in the following, one of the main background sources are semi-electronic charm decays (b.r. $\approx 10\%$ [10]).

In Section 2 the detection strategy employed in this study is outlined and in Section 3 we describe the procedure used for event simulation and reconstruction. In Section 4 we summarize the expected electron identification performance. The interplay between primary interaction vertex reconstruction and identification of displaced tracks is discussed in Section 5. The optimization of the beauty signal selection and the expected sensitivity are reported in Sections 6 and 7. We estimate the expected statistical and systematic errors for a sample of 10^9 inelastic pp events, which is a conservative assumption for a data-taking period of a few months at the nominal luminosity at the ALICE interaction point, $\mathcal{L} \approx 10^{30}$ cm^{-2}s^{-1}. We also estimate the statistical errors, and the covered $p_{\rm t}$ range, for a reduced sample, as could be collected during the first weeks of data-taking at LHC start-up.

2 Background sources and detection strategy

The main sources of background for the signal of beauty-decay electrons are: decays of primary D mesons, which have a branching ratio of $\approx 10\%$ in the semi-electronic channels [10], and have an expected production yield larger by a factor about 20 with respect to B mesons (see Table 1); decays of light mesons (mainly ρ, ω, K) and neutral pion Dalitz decays ($\pi^0 \rightarrow \gamma e^+ e^-$); conversions of photons in the beam pipe or in the inner layers of the ITS; charged pions misidentified as electrons. Figure 1 shows the distributions of the signal and of the different background sources, in transverse impact parameter d_0, defined as the distance of closest approach of the track to the primary vertex in the plane transverse to the beam direction, and in transverse momentum $p_{\rm t}$.

The detection strategy is adapted from that developed for Pb–Pb collisions [11] and is based on two steps:

1. *Electron identification.* The separation of electrons from heavier charged particles relies on a combined selection on specific energy loss $\mathrm{d}E/\mathrm{d}x$, measured in the TPC, and transition radiation, measured in the TRD. The expected performance of this technique will be shown in Section 4.
2. *Impact parameter cut.* Because of the large mean proper decay length (≈ 500 μm) of beauty mesons, their decay electrons have typical displacements of a few hundred microns with respect to the primary vertex. A cut on a minimum value of $|d_0|$ allows to reject a large fraction of the background (see Fig. 1). We have optimized the value of this cut as a function of the transverse momentum in order to minimize the total errors (statistical + systematic, shown in Section 6.3).

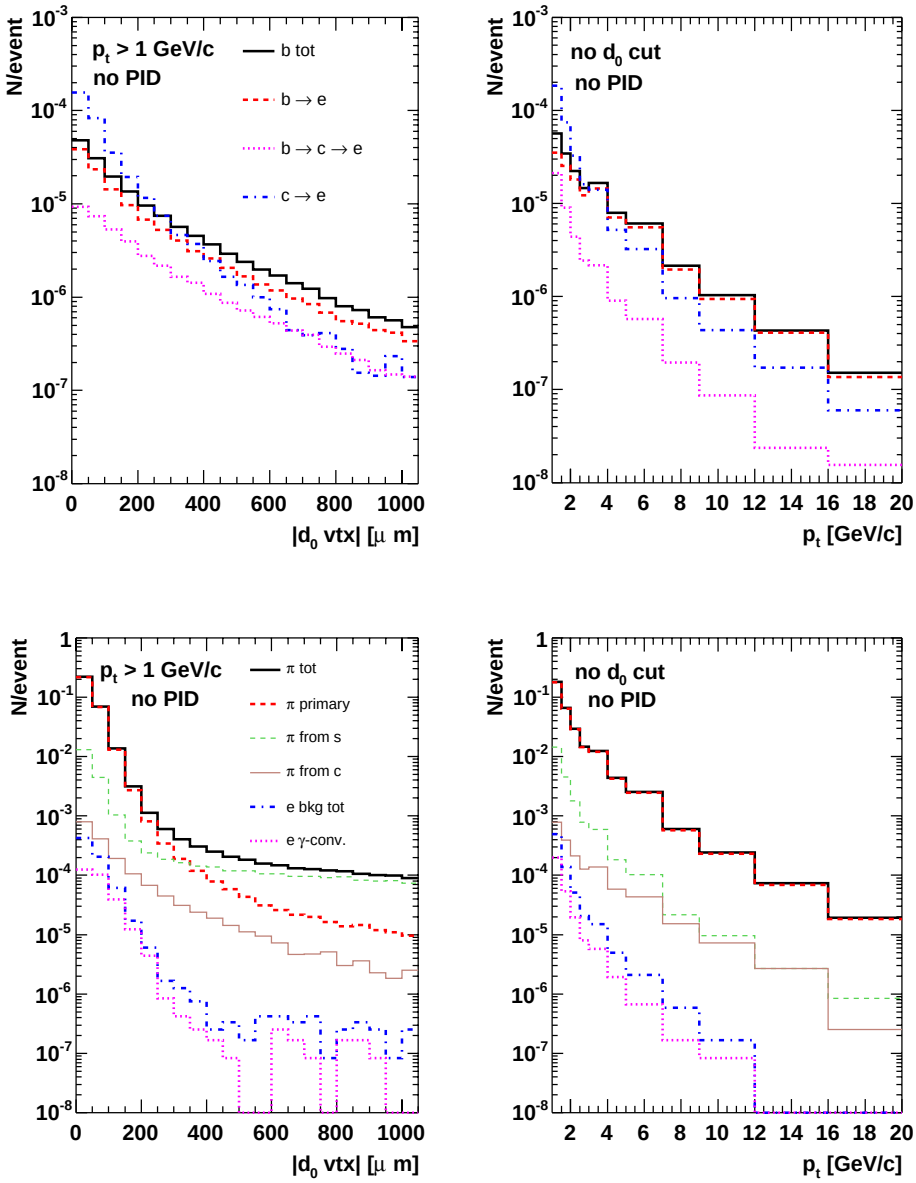

Figure 1: *Beauty and charm decay electrons (top), electrons from other sources and charged pions (bottom), as a function of* $|d_0|$ *(left) and* p_t *(right). Here,* $|d_0|$ *is calculated with respect to the true primary vertex position, known from simulation.*

3 Event simulation and reconstruction

Events were generated using PYTHIA [12]. Large statistics samples are needed in order to study electron transverse momentum distributions up to 15–20 GeV/c, after applying a tight impact parameter cut. We evaluated the required statistics to about 10^7 pp minimum-bias events, 10^6 pp events containing a $c\overline{c}$ pair and 10^6 pp events containing a $b\overline{b}$ pair. To produce such statistics in an acceptable time-frame, we adopted the following fast-simulation techniques: fast detector response in the ITS (a gaussian smearing of the *hit* position is used to obtain the *cluster* position, with a 1% detector inefficiency taken into account) and parametrized response of the Kalman-filter tracking in the TPC (see Ref. [13]).

For the background, we used a sample of 6×10^6 minimum-bias pp events (MSEL=0 option with process ISUB=95, "low-$p_{\rm t}$ scattering", in PYTHIA) at $\sqrt{s} = 14$ TeV. For pp events with a heavy-quark pair, we used the same PYTHIA settings as for minimum-bias events, without forcing heavy-flavour production, but selecting *a posteriori* pp events containing a $\rm c\overline{c}$ or $\rm b\overline{b}$ pair. This approach allows to have a realistic underlying-event multiplicity, as required to perform the primary vertex reconstruction on an event-by-event basis using measured tracks (see Section 5). Since the resulting shapes of the charm and beauty quarks $p_{\rm t}$ distributions are different from those given by NLO pQCD predictions [7] and assumed as the ALICE baseline, we reweighted the decay electrons in order to match the baseline shapes. In order to further speed-up the generation step, in $\rm Q\overline{Q}$ events we required a decay electron in the acceptance of the barrel ($|\eta| < 0.9$) and calculated the proper normalization using low-statistics reference samples. The final statistics amounts to 3.57×10^5 charm events and 4.09×10^5 beauty events, corresponding to 4.6×10^7 and 5.4×10^8 pp minimum-bias events, respectively. The samples, for background and for pp events with a heavy-quark pair, were normalized to one pp event.

Event reconstruction was performed using the parametrized tracking response in the TPC and the standard Kalman-filter tracking in the ITS. Tracks were required to have an assigned cluster in each of the six ITS layers. The value of the magnetic field in the barrel was set to 0.4 T. The physical track reconstruction efficiency (number of reconstructed tracks in TPC and ITS relative to the number of generated particles in the acceptance) for $p_{\rm t} > 2$ GeV/c is about 65%, 70% and 75%, for kaons, pions and electrons, respectively. An additional efficiency factor of 75% is introduced to account for the probability that the track is also prolonged to the TRD, placed outside the TPC.

4 Electron identification in TPC and TRD

Electrons can be efficiently separated from hadrons by combining the PID capabilities of the TPC, based on specific energy loss $\mathrm{d}E/\mathrm{d}x$, and of the TRD, specifically devoted to electron identification via the transition radiation technique. In this study we assume for the pp case the same electron PID performance as expected in Pb–Pb collisions [11] (see Fig. 2). Under the assumption of $e_{\rm eff}^{\rm TRD} = 90\%$ electron identification probability, the TRD is expected to reject 99% of the charged pions ($\pi_{\rm eff}^{\rm TRD} = 10^{-2}$ misidentification probability) and fully reject heavier charged hadrons, for $p > 1$ GeV/c. Using the $\mathrm{d}E/\mathrm{d}x$ information from the TPC, the probability of pion misidentification can be further reduced by a factor $\sim 10^{-2}$ at low momentum. As the momentum increases and charged pions approach the Fermi plateau in $\mathrm{d}E/\mathrm{d}x$, the additional pion rejection from the TPC decreases and becomes marginal at $p \simeq 10$ GeV/c.

Figure 3 shows the effect of electron identification on our samples. Without identification, charged pions dominate the electron sample at all transverse momenta. The filter provided by the TPC and the TRD is expected to reduces the pion contamination by a factor 6×10^{-5} at $p_{\rm t} = 2$ GeV/c and 7×10^{-3} at $p_{\rm t} = 18$ GeV/c.

5 Primary vertex reconstruction and selection of displaced tracks

Due to the TPC and SDD (Silicon Drift Detectors) speed limitations, during LHC proton–proton runs, the luminosity at the ALICE interaction point has to be kept below $\mathcal{L}_{\rm max} \simeq 3 \times 10^{30}$ cm^{-2}s^{-1} [1]. When the machine luminosity will be larger than this value (the design luminosity is $\mathcal{L}_0 \approx 10^{34}$ cm^{-2}s^{-1}), the luminosity at the ALICE interaction point will have to be reduced, most likely by refocusing the beams, i.e. by enlarging their transverse size from the nominal $\sigma_{x,y} \simeq 15$ μm to ~ 150 μm. The primary vertex position

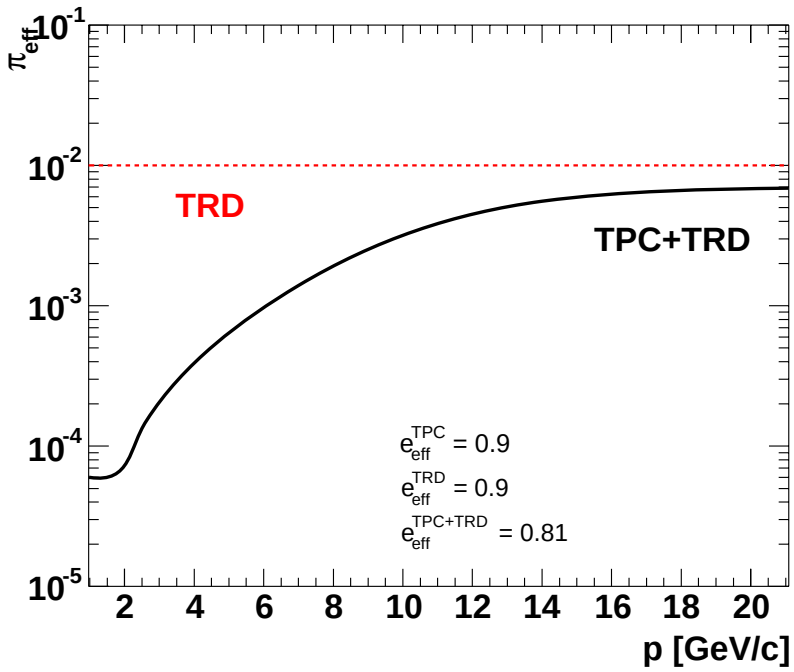

Figure 2: *Probability* π_{eff} *to misidentify a charged pion as electron, as a function of the momentum, with TRD only and combining TPC and TRD. PID cuts on* $\mathrm{d}E/\mathrm{d}x$ *and transition radiation are set such that the probability* e_{eff} *for correct electron identification is 90% in each of the two detectors.*

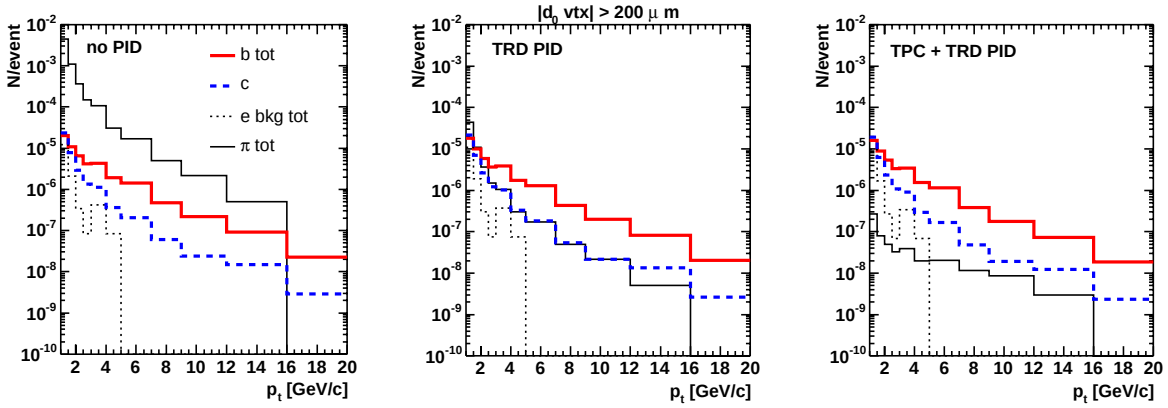

Figure 3: *Yields of electron-tagged tracks as a function of* p_{t} *for the various sources with no PID, with PID using only the TRD and using TPC and TRD combined. For illustration, the cut* $|d_0| > 200$ μm *is applied, with* d_0 *calculated with respect to the true primary vertex position.*

will be reconstructed on an event-by-event basis, using measured tracks, with an expected resolution of about 90 μm in x and y on average [14]. Due to the large beam size, the event-by-event estimate cannot be improved by averaging over many events.

The current algorithm for vertex reconstruction in pp is based on two steps [14]:

1. Vertex Finding: a first estimate of the vertex position is obtained using track pairs.

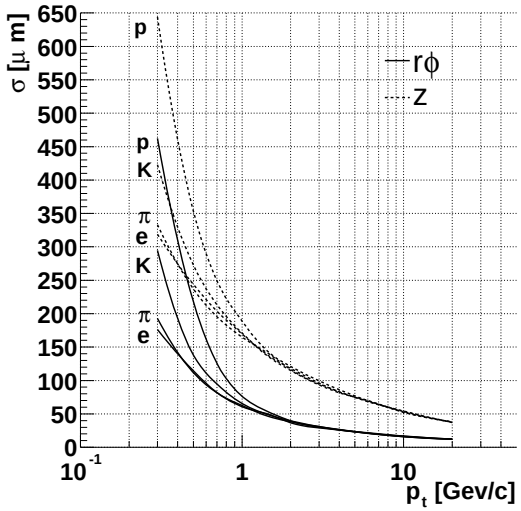

Figure 4: *Impact parameter resolutions (with respect to the generated primary vertex position) for electrons, pions, kaons and protons as a function of the transverse momentum [15].*

2. Vertex Fitting: tracks are propagated to the position estimated in the first step and the optimal estimate of the vertex position is obtained via a fast fitting algorithm. In this step a cut on the maximum single-track contribution to the vertex χ^2 is applied in order to remove secondary tracks from the fit.

In order to further improve the precision on the primary vertex position and to optimize the strategy for selecting displaced tracks, we study here different methods for preselecting the tracks to be used for the vertexing procedure. The methods are:

- ALL: the vertex is determined once per event using all tracks (no preselection);
- OTHERS: the primary vertex is recalculated for each candidate displaced track, using the *other* tracks in the event;
- $1\,\sigma$, $3\,\sigma$, $5\,\sigma$: the vertex is determined once per event using the tracks with transverse impact parameter $|d_0| < n\,\sigma(p_{\rm t})$, where d_0 is calculated with respect to the "ALL" vertex and $\sigma(p_{\rm t})$ is the parametrized $p_{\rm t}$-dependent $r\phi$ track-position resolution (see Fig. 4 [15]).

Figure 5 shows the impact parameter distributions of the various sources of signal (charm-decay and beauty-decay electrons) and background (background electrons and electron-tagged pions), as obtained from the different methods. The ideal case "VTX" with the true primary vertex position known from the simulation is also shown. The results from the $5\,\sigma$ method are not shown because they are very similar to those of the $3\,\sigma$ method. It can be seen that the two methods that best resemble the ideal case are $1\,\sigma$ and $3\,\sigma$, in the two lower panels of Fig. 5.

We also examined (Fig. 6) the distributions of the modulus of the residual $|d_0 - d_0^{\rm True}|$ between the transverse impact parameter, evaluated with the different methods, and its true value. Again, the $1\,\sigma$ and $3\,\sigma$ methods approach most closely the ideal case "VTX", albeit the differences between the various methods are small.

An additional parameter to be considered for the choice of the optimal method, is the amount of beauty-decay electron tracks that are "discarded" because less than three tracks are left in the event after the preselection, thus preventing to reconstruct the primary vertex position. The fraction of *retained* signals for the different track-preselection

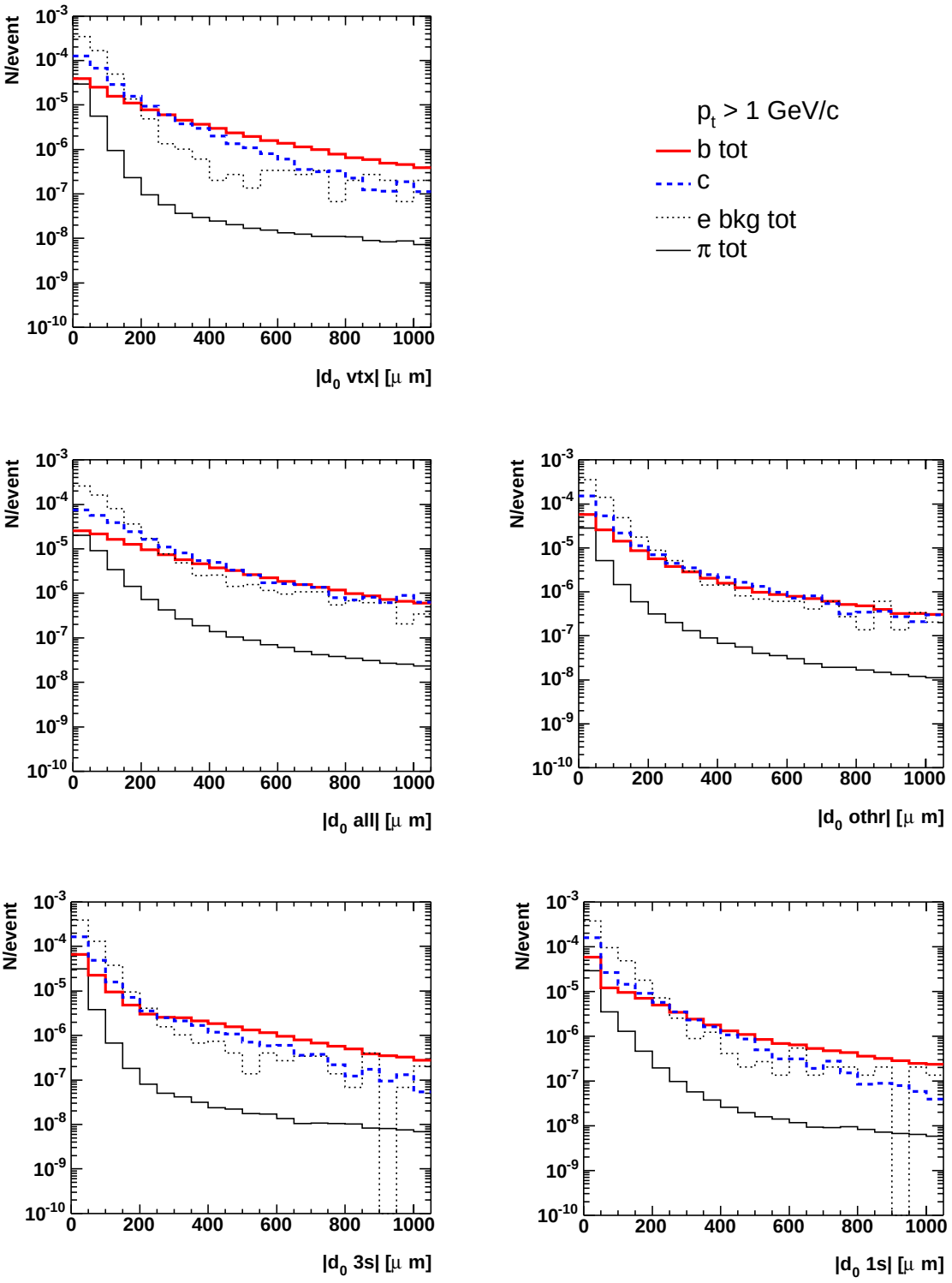

Figure 5: *Distributions of the absolute value of the impact parameter for identified electrons from beauty decays, from charm decays, identified electrons from the background and pions tagged as electrons. The cut* $p_t > 1$ GeV/c *is applied. The panels differ in the method used for primary vertex track-preselection, as explained in the text.*

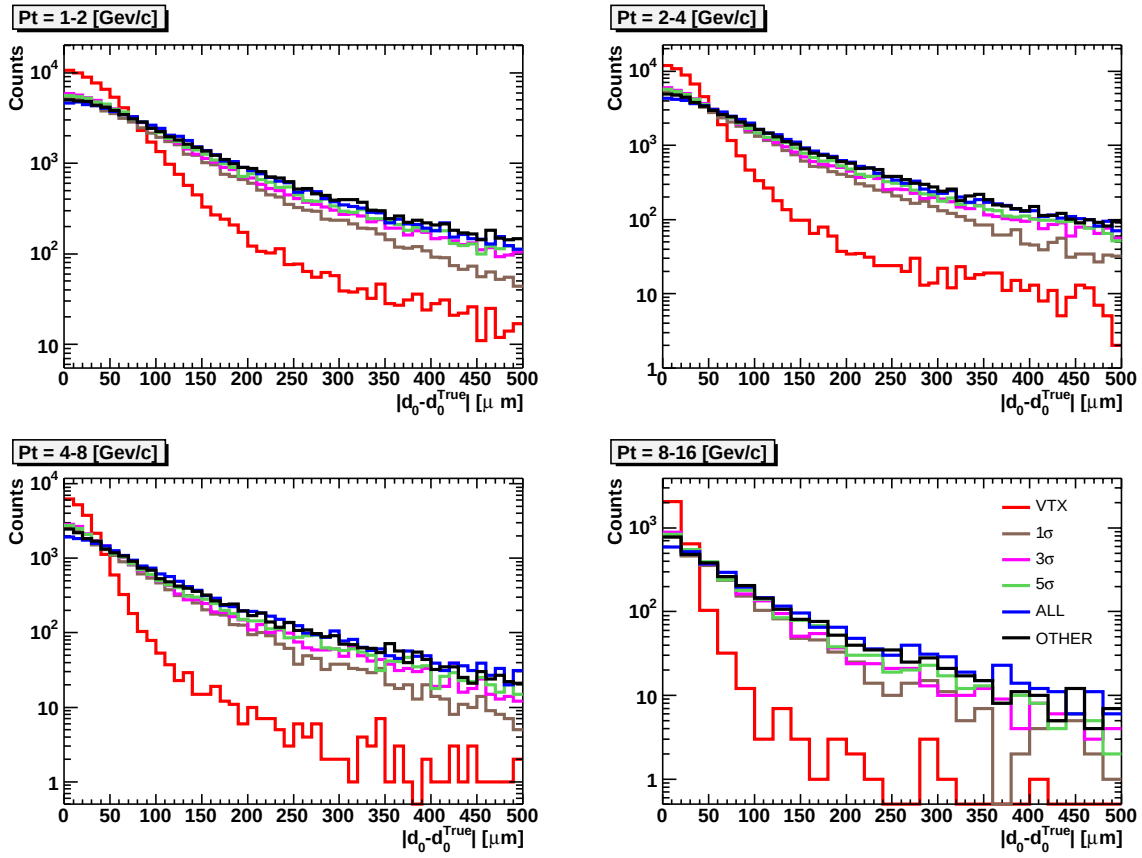

Figure 6: *Distributions of* $|d_0 - d_0^{True}|$ *for electron–tagged tracks for the different methods used for primary vertex track-preselection.*

methods is shown in Fig. 7: the $1\,\sigma$ and $3\,\sigma$ methods discard about 15% and 5% of the beauty signal, respectively.

From our analysis we conclude that the $3\,\sigma$ method is optimal for beauty detection via displaced electrons.

6 Analysis

As mentioned before, the detection strategy relies on the different shapes of the transverse momentum and impact parameter distributions for electrons from beauty, from charm, and for the different background contributions (see Fig. 1). After the filter of electron identification, a $p_{\rm t}$-dependent impact parameter cut will be applied; then, the residual background contributions have to be estimated and subtracted. For a given electron $p_{\rm t}$ interval, the value of the d_0 cut should be optimized in order to minimize the total error (statistical and systematic) on the number of beauty-decay electrons in the interval. Therefore, before presenting the analysis on the cut optimization, we describe in detail the procedure we envisage to use for the extraction of the beauty-decay electron production cross section, also discussing the expected error contributions.

6.1 Extraction of the electron-level cross section

In a given $p_{\rm t}$-bin, the number N of counted "electrons" will be the sum of different contributions: $N = N_{\rm b}$ (beauty) + $N_{\rm c}$ (charm) + $N_{\rm bkg}$ (background e and misidentified π). The cross section will be obtained by the following four-step procedure.

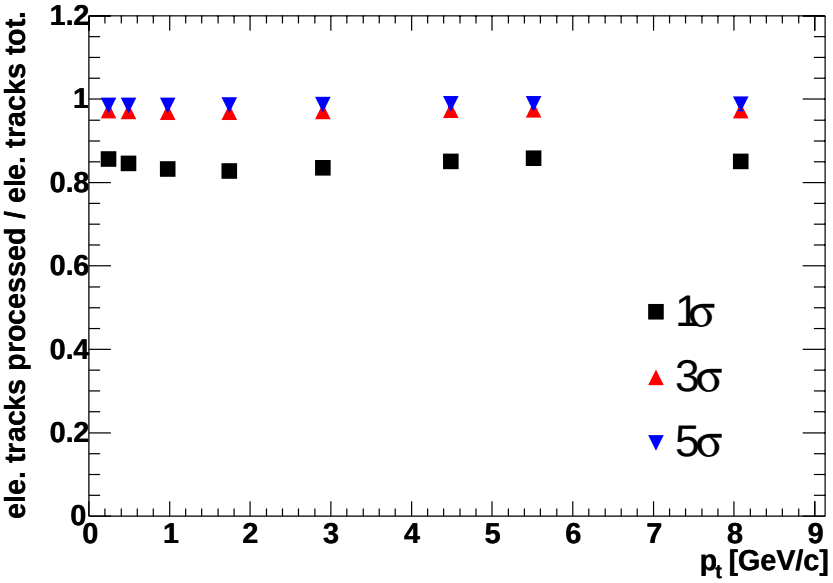

Figure 7: *Fraction of retained beauty-decay electron tracks for the different methods used for primary vertex track-preselection (see text for details).*

1. Subtraction of charm-decay electrons. We plan to use the cross section for D^0 mesons, measured in ALICE in the $\mathrm{K}^-\pi^+$ decay channel [16, 17], to estimate the N_c contribution.
2. Subtraction of the remaining background electrons and misidentified pions, on the basis of Monte Carlo simulations tuned on the measured light-flavour hadron production.
3. Correction of the number of beauty electrons, $N_\mathrm{b} = N - N_\mathrm{c} - N_\mathrm{bkg}$, for efficiency (tracking, electron ID, d_0 cut) and acceptance: $\mathrm{d}N_\mathrm{b}^\mathrm{corr}/\mathrm{d}y = N_\mathrm{b}/\epsilon$. The correction will be done via Monte Carlo and its stability will be checked by varying the value of the cut.
4. Normalization of the corrected yield to a cross section for beauty-decay electrons $\mathrm{d}\sigma^{e\,\mathrm{from\,b}}/\mathrm{d}y = \sigma_\mathrm{pp}^\mathrm{inel} \cdot \mathrm{d}N_\mathrm{b}^\mathrm{corr}/\mathrm{d}y$.

6.2 Experimental uncertainties

Each step of the outlined procedure introduces an error contribution.

- **Statistical error.** For a given p_t-bin, with N_b electrons from beauty, N_c electrons from charm, N_bkg electrons from background, the relative statistical error on the beauty signal (N_b), after the subtractions of steps 1 and 2, is

$$\left.\frac{\delta N_\mathrm{b}}{N_\mathrm{b}}\right|_\mathrm{stat} = \frac{\sqrt{N_\mathrm{b} + N_\mathrm{c} + N_\mathrm{bkg}}}{N_\mathrm{b}}\,. \tag{1}$$

- **Systematic error from Monte Carlo corrections.** The error from MC correction (acceptance, efficiency of track reconstruction, efficiency of PID and d_0 cut) is assumed to be 10% over the whole p_t range, although it is, in principle, p_t-dependent.
- **Systematic error from uncertainties on charm and background electrons to be subtracted.** Once the relative errors on charm and background are known,

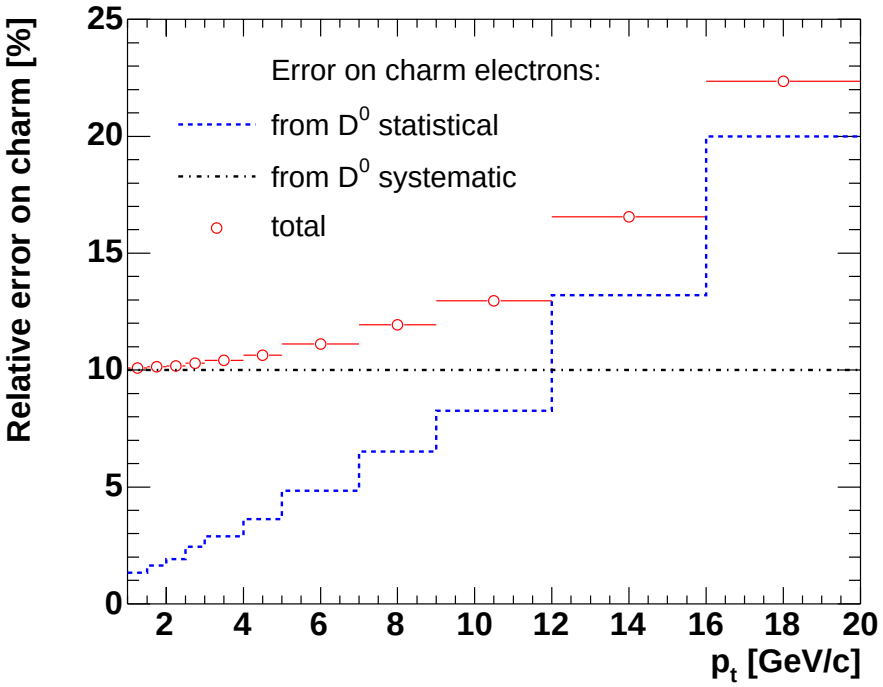

Figure 8: *Relative error on charm-decay electrons as a funcion of* $p_{\rm t}$*, estimated by propagating to the electron level the statistical and systematic errors on the measurement of the* $\rm D^0$ *production cross section in the* $\rm D^0 \to K^-\pi^+$ *channel.*

the two contributions to the final relative error are proportional to the charm-to-beauty ratio and background-to-beauty ratio, respectively:

$$\left.\frac{\delta N_{\rm b}}{N_{\rm b}}\right|_{\rm syst.subtr.} = \sqrt{\left(\frac{N_{\rm c}}{N_{\rm b}}\frac{\delta N_{\rm c}}{N_{\rm c}}\right)^2 + \left(\frac{N_{\rm bkg}}{N_{\rm b}}\frac{\delta N_{\rm bkg}}{N_{\rm bkg}}\right)^2}\,. \qquad (2)$$

The electron distribution from charm decays, to be subtracted, will be estimated from the measurement of $\rm D^0 \to K^-\pi^+$. The method for evaluating the distribution to be subtracted and the relative error on charm decays follows the same procedures as in the Pb-Pb case. It is described in [6]. The resulting relative error on charm ($\delta N_{\rm c}/N_{\rm c}$) is shown in Fig. 8 for the pp case. The relative error on the background ($\delta N_{\rm bkg}/N_{\rm bkg}$) is assumed to be 10%, $p_{\rm t}$-independent.

- **Systematic error on the proton–proton inelastic cross section.** A 5% error is expected on the measurement of the pp inelastic cross section with ALICE [1].

6.3 Optimization of selection cuts

The impact parameter cut affects the fraction of beauty-decay electrons in the sample, and therefore the statistical error (see Eq. (1)) and the systematic error from subtractions, via the ratios $N_{\rm c}/N_{\rm b}$ and $N_{\rm bkg}/N_{\rm b}$ (see Eq. (2)). We analyzed, in bins of $p_{\rm t}$, the minimum-d_0 dependence of statistical and systematic errors. As an example, in Fig. 9 we present this dependence for three bins: in each row, the left-most and central panels show the three ratios affected by the cuts ($N_{\rm b}/N$, $N_{\rm c}/N_{\rm b}$ and $N_{\rm bkg}/N_{\rm b}$) and the right-most panel summarizes the relative errors on the beauty-decay electrons cross section, as a function of the cut value.

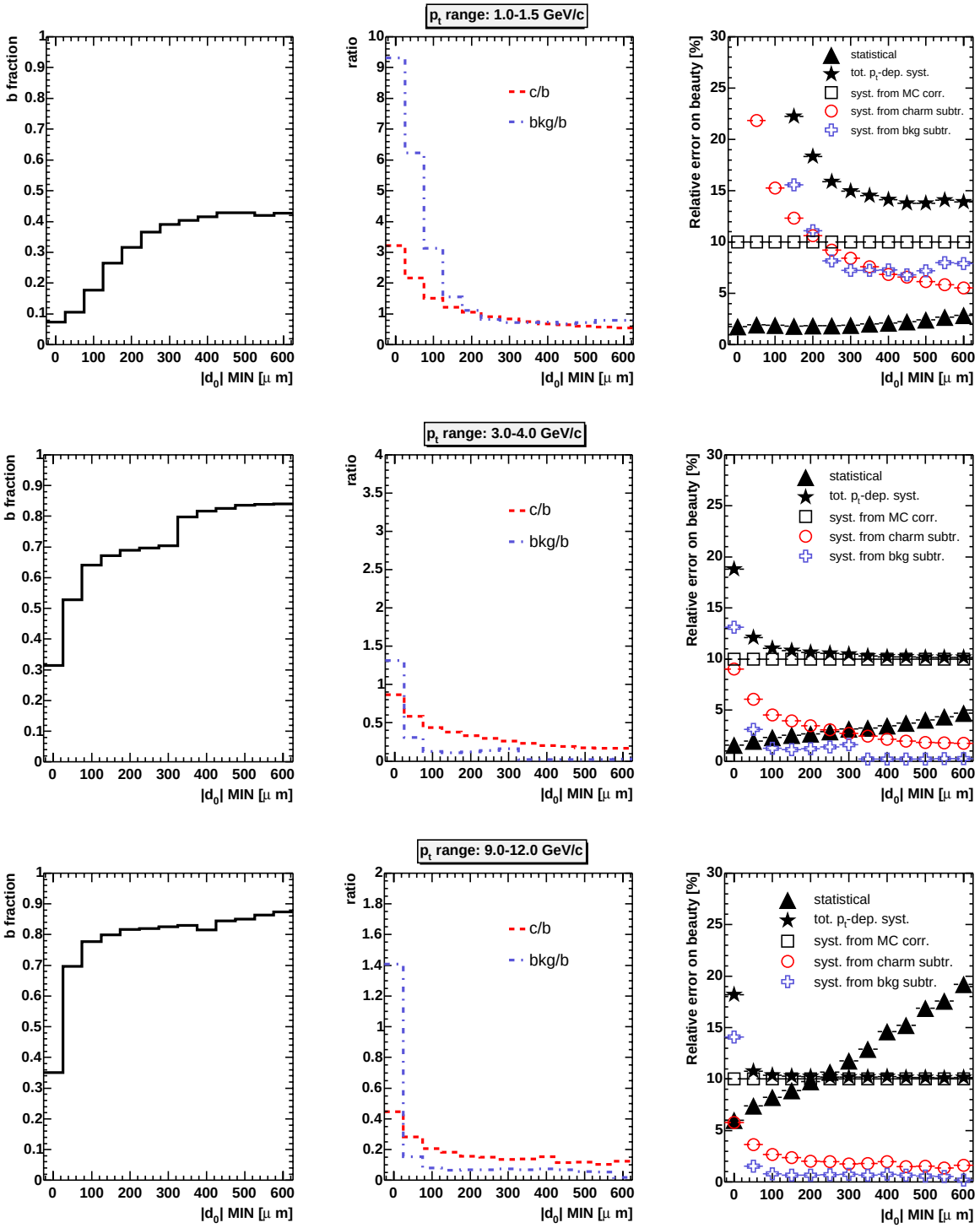

Figure 9: *Left: fraction of beauty-decay electrons,* $N_{\rm b}/(N_{\rm b}+N_{\rm c}+N_{\rm bkg})$. *Center: fraction of charm-decay electrons over beauty-decay electrons,* $N_{\rm c}/N_{\rm b}$, *and of background electrons over beauty-decay electrons,* $N_{\rm bkg}/N_{\rm b}$. *Right: summary of the error contributions. All variables are shown as a function of the minimum impact parameter. The three rows refer to different* $p_{\rm t}$*-bins.*

The systematic error from the charm and background subtractions is relevant only at low $p_{\rm t}$, where the non-beauty contributions dominate the sample, and it decreases for

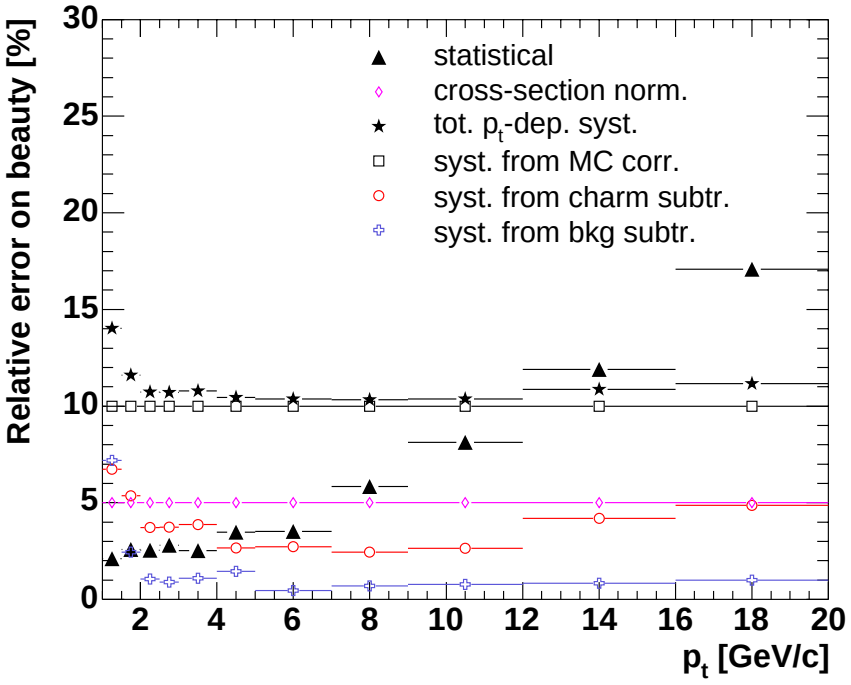

Figure 10: *Summary of the error contributions as a function of* p_{t}. *A statistics of* 10^9 *pp events is assumed.*

increasing cut values. The statistical error is small at low p_{t}, also for large values of the d_0 cut, while it becomes the dominant contribution at high p_{t} and for d_0 cuts larger than 100–200 μm. For each p_{t}-bin, we selected the cut value that minimizes the quadratic sum of statistical and systematic errors. Table 2 shows the chosen cut values and the resulting errors.

7 Results

In Figs. 10 and 11 we show the summary of the expected errors and the sensitivity for the measurement of the production cross section of beauty-decay electrons, for a statistics of

Table 2: *Values of the transverse impact parameter cut and the resulting systematic and statistical errors.*

p_{t} [GeV/c]	$\lvert d_0^{min}\rvert$ [μm]	Statistical error [%]	p_{t}-dep. systematic error [%]
1.0–1.5	400	2.1	14.0
1.5–2.0	400	2.6	11.6
2.0–2.5	300	2.5	10.7
2.5–3.0	200	2.8	10.7
3.0–4.0	150	2.5	10.8
4.0–5.0	150	3.5	10.4
5.0–7.0	100	3.6	10.4
7.0–9.0	100	5.8	10.3
9.0–12.0	100	8.1	10.4
12.0–16.0	50	11.9	10.9
16.0–20.0	50	17.1	11.2

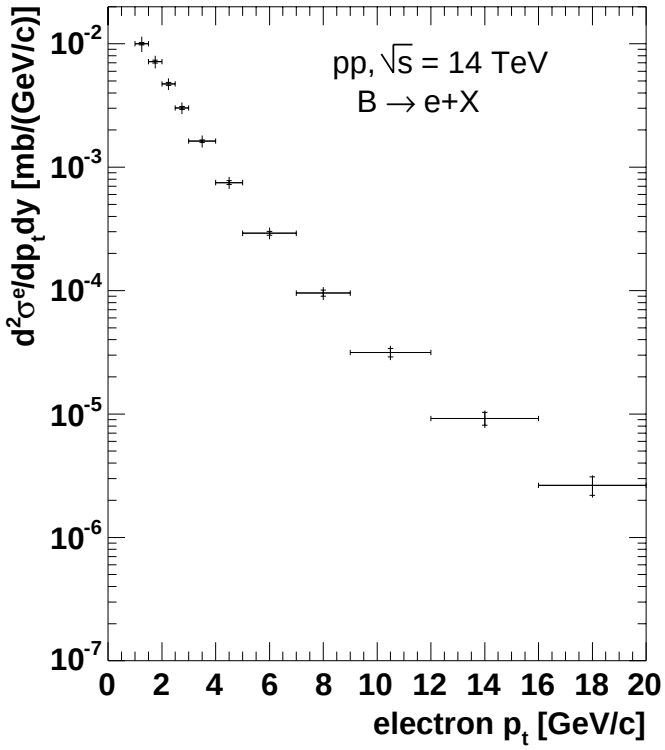

Figure 11: *Differential cross section for beauty-decay electrons per pp collision as a function of $p_{\rm t}$, as measurable with 10^9 events; statistical errors (inner bars) and quadratic sum of statistical and $p_{\rm t}$-dependent systematic errors (outer bars) are shown; the 5% normalization error is not shown.*

10^9 minimum-bias proton–proton events.

We tested the possibility to infer the $p_{\rm t}^{\rm min}$-differential cross section for beauty mesons, $\mathrm{d}\sigma^B(p_{\rm t} > p_{\rm t}^{min})/\mathrm{d}y$, from the electron-level cross section using a procedure similar to that developed by the UA1 Collaboration [18]. The method, described in detail in Refs. [5, 6, 11], is based on Monte Carlo simulation and it relies on the fact that the B meson decay kinematics, measured and studied in several experiments, is well understood. It has been shown [11] for the Pb-Pb case that, if electrons with $p_{\rm t} > 2$ GeV/c are used (below this limit, the correlation between the electron and B meson momenta is very poor), the additional systematic error is negligible with respect to the systematic uncertainties already present at the electron level.

Figure 12 presents the expected ALICE performance for the measurement of the $p_{\rm t}^{min}$-differential cross section of B mesons, $\mathrm{d}\sigma^B(p_{\rm t} > p_{\rm t}^{min})/\mathrm{d}y$ vs. $p_{\rm t}^{min}$ averaged in the range $|y| < 1$. For illustration of the sensitivity in the comparison to pQCD calculations, we report in the same figure the predictions and the theoretical uncertainty bands from three approaches [19]: collinearly-factorized Fixed Order Next-to-Leading Order (FO NLO), as implemented in the HVQMNR code [7], Fixed Order Next-to-Leading Log (FONLL) [20] and $k_{\rm t}$-factorization, as implemented in the CASCADE code [21]. It can be seen that the expected ALICE performance for 10^9 events will provide a meaningful comparison with pQCD predictions.

As mentioned in the Introduction, the statistics of 10^9 pp events is expected to be accumulated in a run at nominal LHC luminosity ($\sim 10^{34}$ cm^{-2}s^{-1} but it will be lowered

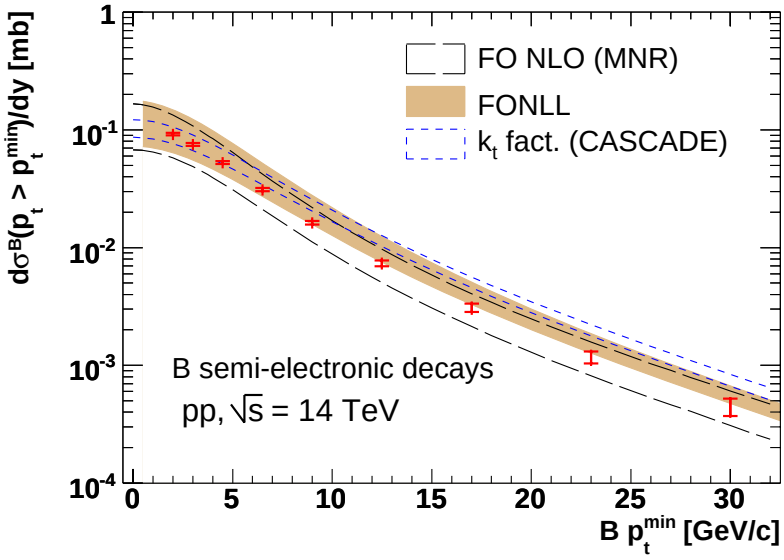

Figure 12: *Differential cross section for B meson production as it can be measured with* 10^9 *pp minimum-bias events. Statistical errors (inner bars) and quadratic sum of statistical and* p_t*-dependent systematic errors (outer bars) are shown; the 9% normalization error is not shown. The theoretical predictions from the three pQCD calculations (see text), with their uncertainties are also shown for comparison with the expected experimental sensitivity.*

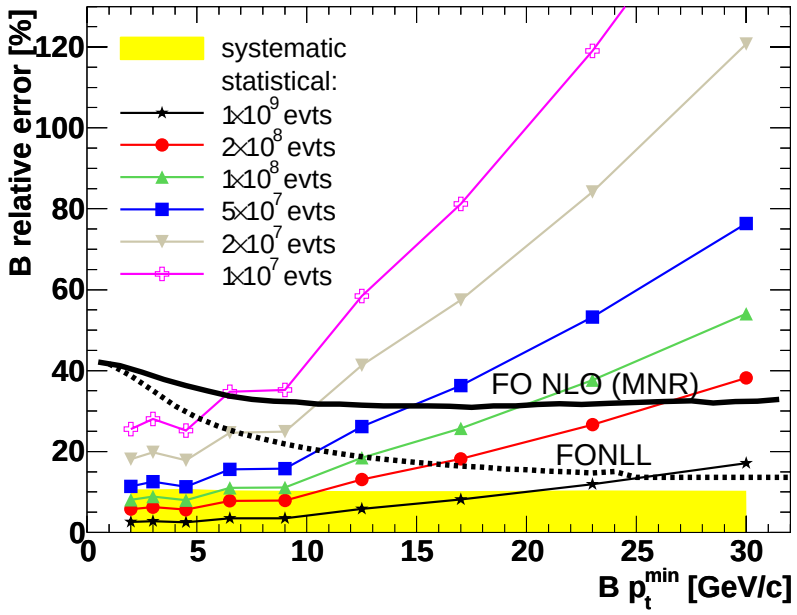

Figure 13: *Comparison between statistical relative error on beauty hadron cross-section as a function of* p_t^{min} *in different scenarios of statistics and theoretical uncertainties for FONLL and FONLO calculation.*

at the ALICE Interaction Point to about $\sim 10^{30}$ cm^{-2}s^{-1}) of about seven months. During the first few weeks after LHC start-up, the luminosity is expected to be much lower than

the nominal value, and it should be of the order of the maximum luminosity at which ALICE can take data ($\sim 10^{30}$ cm^{-2}s^{-1}). Therefore, soon after the start-up, it should be possible to collect data at the nominal rate. A sample of up to 10^8 events may be accumulated in about a month. However, depending on the time-line of installation of the TRD detector modules, the electrons statistics could be further reduced to a sample equivalent to a few 10^7 pp events. We have extrapolated the results of our study to lower-statistics, albeit without changing the cuts. In Fig. 13 we show the relative statistical errors on the beauty cross section for different sample sizes. By comparing the statistical error with the systematic error and with the theoretical uncertainty bands, we can argue that a significant measurement of (low-$p_{\rm t}$) beauty production is possible with data from the first few weeks of run at LHC.

8 Conclusions

In the present study we investigated the performance of ALICE for the measurement of beauty production, via displaced electrons, in proton–proton collisions at $\sqrt{s} = 14$ TeV. This measurement is a good test for perturbative QCD in a new energy domain. It will also be essential for a comparison with the corrisponding measurements in Pb–Pb collisions, for example for the investigation of b-quark in-medium energy loss.

The detection strategy investigated here relies on the selection of displaced tracks identified as electrons. The identification is done combining TRD–TPC information, while the displacement is evaluated using the transverse impact parameter with respect to the primary vertex. In pp collisions at ALICE, the primary vertex position has to be reconstructed on an event-by-event basis using measured tracks. Thus, we optimized the preselection criterion for tracks to be used in the vertex reconstruction, in order to improve the impact parameter resolution: the vertex is first found using all tracks, then a second iteration is performed using only tracks within $3\,\sigma$ from the first determination of the vertex. For σ we currently use the parametrized transverse track-position resolution as a function of $p_{\rm t}$, but we plan to further develop the procedure by extracting σ directly from the covariance matrix of each track. We also plan to include the uncertainty on the reconstructed primary vertex position in the selection of the tracks.

Our results indicate that ALICE can provide a measurement of B meson production in the transverse momentum range 2–30 GeV/c with errors that are comparable to the theoretical uncertainties of pQCD calculations. A preliminary investigation suggests that a significant measurement could be carried out during the first few weeks of LHC running, even with a partial acceptance coverage for the Transition Radiation Detector.

References

[1] ALICE Collaboration, ALICE Physics Performance Report, Volume I, CERN/LHCC 2003-049, J. Phys. **G30** (2004) 1517.

[2] N. Armesto, A. Dainese, C.A. Salgado and U.A. Wiedemann, Phys. Rev. **D71** (2005) 054027.

[3] M. Cacciari, arXiv:hep-ph/0407187.

[4] M. L. Mangano, AIP Conf. Proc. **753** (2005) 247 [arXiv:hep-ph/0411020].

[5] P. Crochet, R. Guernane, A. Morsch and E. Vercellin, ALICE Internal Note ALICE-INT-2005-018 (2005).

[6] ALICE Collaboration, ALICE Physics Performance Report, Volume II, CERN/LHCC 2005-030.

[7] M. L. Mangano, P. Nason and G. Ridolfi, Nucl. Phys. **B373** (1992) 295.

[8] H.L. Lai *et al.*, CTEQ Coll., Eur. Phys. J. **C12** (2000) 375.
[9] A.D. Martin, R.G. Roberts, W.J. Stirling and R.S. Thorne, Eur. Phys. J **C4** (1998) 463.
[10] S. Eidelmann *et al.*, Particle Data Group Coll., Phys. Lett. **B592** (2004) 1.
[11] F. Antinori, A. Dainese, M. Lunardon and R. Turrisi, ALICE Internal Note ALICE-INT-2005-033 (2006).
[12] T. Sjöstrand, P. Edén, C. Friberg, L. Lönnblad, G. Miu, S. Mrenna and E. Norrbin, Computer Phys. Commun. **135** (2001).
[13] A. Dainese and N. Carrer, ALICE Internal Note ALICE-INT-2003-011 (2003).
[14] A. Dainese and M. Masera, ALICE Internal Note ALICE-INT-2003-027 (2003).
[15] A. Dainese and R. Turrisi, ALICE Internal Note ALICE-INT-2003-028 (2003).
[16] N. Carrer, A. Dainese and R. Turrisi, J. Phys. **G29** (2003) 575.
[17] A. Dainese, Ph.D. Thesis, Università degli Studi di Padova (2003), arXiv:nucl-ex/0311004.
[18] C. Albajar *et al.*, UA1 Coll., Phys. Lett. **B213** (1988) 405;
C. Albajar *et al.*, UA1 Coll., Phys. Lett. **B256** (1991) 121.
[19] J. Baines *et al.*, arXiv:hep-ph/0601164, Subgroup contribution to the proceedings of the "HERA and the LHC" workshop.
[20] M. Cacciari, M. Greco and P. Nason, JHEP **9805** (1998) 007 [arXiv:hep-ph/9803400];
M. Cacciari, S. Frixione and P. Nason, JHEP **0103** (2001) 006 [arXiv:hep-ph/0102134].
[21] H. Jung, Comput. Phys. Commun. **143** (2002) 100 [arXiv:hep-ph/0109102].